J. theor. Biol. (1986) **123**, 81-101

A Mathematical Model of Pattern Formation

EDUARDO J. CHICHILNISKY†

Princeton University, Princeton, N.J., U.S.A.

(*Received* 14 *January* 1986, *and in revised form* 30 *April* 1986)

This paper presents an explicit mathematical model describing pattern formation in monolayer epithelia. The approach is a generalization of the equations describing soap bubble configurations (Plateau, 1873; Thompson, 1917; Almgren & Taylor, 1976) that allows adjacent cells to adhere with differing intensities (Steinberg, 1962, 1978). The model is a system of simultaneous non-linear equations that considers cell-cell interactions in a two-dimensional sheet. The implementation involves using the equations of the model to predict explicitly the energy-minimizing configuration of a system of cells, based on the adhesivity of their membranes. The model can thus be used to explore the effects of varying adhesions on the dynamics of pattern formation. Following Chichilnisky (1985), such a descriptive system is introduced in this paper, and its predictive properties explored.

1. Introduction

The parallels between the configurations adopted by soap bubbles and simple systems of cells have long been noted (Thompson, 1917), and the equations governing these configurations have been explicitly formulated (Almgren & Taylor, 1976). However, soap bubbles are limited analogs for cells undergoing morphogenesis. Since all bubble "membranes" (soap films) are identical, the interfacial interactions between neighbouring bubbles are identical and little complexity can be generated by the system. The paramount importance of differing interfacial interactions between neighbouring cells during morphogenesis is evident in Steinberg's (1962, 1978) observation that mixtures of dissociated embryonic cells sort out according to a hierarchy of adhesivities. Applications of Steinberg's differential adhesion hypothesis have largely concerned morphogenetic events in which cells flow freely with respect to each other in a liquid-like fashion, and in these systems, the predictions of the hypothesis are amply verified.

Many interesting biological patterns emerge in epithelial monolayers in which cells are more constrained; typically epithelial cells are anchored at their apical and basal poles and are not free to move significantly with respect to their neighbors. The model presented here allows the application of Steinberg's hypothesis to the more restricted cell behaviors prevailing in epithelial sheets. From a simultaneous

† This paper summarizes the results of my senior thesis in the Department of Mathematics, Princeton University (Chichilnisky, 1985). I am deeply indebted to Dr. D. F. Ready who provided me with the continuous intellectual stimulation, comments, and suggestions that led to the development of this model. I am also grateful to Professors A. Majda, W. Thurston, S. Childress, J. K. Percus, J. Taylor, G. Heal, and G. Chichilnisky for many comments and criticisms. This work was supported by an N.S.F. grant to D. F. Ready.

0022-5193/86/210081+21 $03.00/0

consideration of the geometrical constraints imposed by the soap bubble-like behavior of cells and the non soap bubble-like differential adhesivities between cells, the model provides an explicit description of the configuration that a system of interacting cells will assume.

The model is a generalization of the classical equations describing soap bubble configurations. Proceeding from Plateau's observation that three and only three bubbles meet at any junction within a two-dimensional array of bubbles, a system of simultaneous non-linear equations is developed which includes a mathematical formulation of Steinberg's differential adhesion hypothesis. Using a measure of the adhesive properties of the cell membranes as the only exogenous variables, the model predicts the shape and contacts of each cell in the system. The equilibrium configuration of a system of cells is described by the minimum-energy solution of the equations. With the plausible assumption that intracellular adhesivities can change with time during development, the model can predict a series of equilibrium configurations of a system of cells, and thus describe the dynamics of morphogenesis.

The procedure adopted for predicting cell configurations is simple. First, we set out explicitly all possible contact configurations of the system of cells satisfying a Plateau condition of three-way contacts (these configurations typically number few). Next, we use the equations of the model to predict explicitly the cell shapes associated with each contact configuration, and a corresponding measure of free-energy of the system. Choosing the configuration with lowest energy as the most likely, we obtain a precise prediction of cell configurations based only on membrane adhesivity. Allowing membrane adhesivity to vary with time (i.e. during development), we can use the model to understand the effects of differential membrane adhesivity on the dynamics of pattern formation.

2. The Model

DESCRIBING THE SYSTEM

Piecewise circular closed curves in the plane offer a simple yet accurate and physically justifiable way to describe interfaces between cells of a monolayer epithelium (Chichilnisky, 1985).† Such a curve with n "sides" is described by the following parameters:

(1) n points in the plane—vertices of the figure.

(2) n real numbers—the curvature of each "side", where the curvature is the inverse of the radius of curvature, and a curvature of zero describes a straight connecting segment.

This convention defines each side of a cell to only within two degrees of freedom: a circular arc may curve to either side of the segment connecting the endpoints,

† Other descriptions exist, such as one involving Voronoi polygons (Sulsky 1984), which allow a fairly accurate visual representation of cell membranes. However, the description by circular segments has the advantage of incorporating the physical notion of a homogeneous membrane separating two fluids with a pressure differential (see Fig. 7). While neither the polygonal nor the piecewise circular construction can accurately model the microscopic properties of a cell membrane, the latter description combines algebraic simplicity with an underlying physical justification.

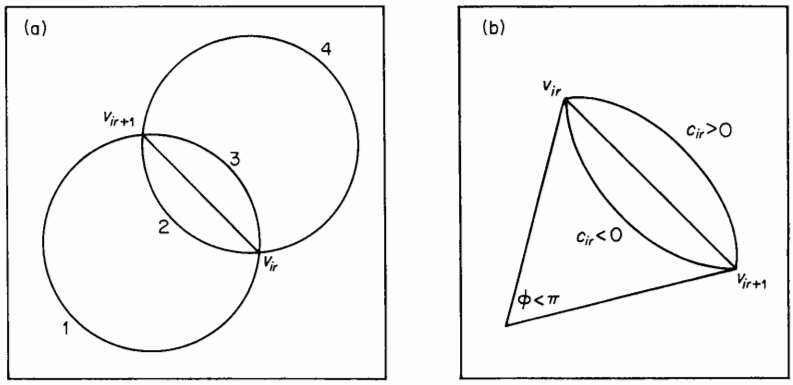

FIG 1 (a). Ambiguity in definition of an arc. (b). Sign and angle conventions to eliminate ambiguity.

and each may have an arc of more or less than π (Fig. 1(a)). To establish conventions that will uniquely describe the side of a cell we first postulate that a positive curvature indicates that the connecting arc curves to the left of the connecting segment (as viewed from the beginning endpoint), a negative value indicating curvature to the right. Second, we will demand that all circular arcs have measure at most π (Fig. 1(b)). The latter assumption is consistent with many soap-bubble configurations (the most notable exception being a two-bubble junction) and can easily be altered to accomodate some arcs of measure greater than π. With these conventions, (1) and (2) above uniquely describe the side of a cell in our system.

Definition: The i^{th} cell C_i in our systems of cells is given by n distinct points in the plane (vertices) and n real numbers (curvatures)

$$\text{vertices:} \quad v_{i1}, \ldots, v_{in}$$

$$\text{curvatures:} \quad c_{i1}, \ldots, c_{in}$$

where $|c_{ir}|$ is the curvature of the arc connecting v_{ir} and v_{ir+1}, with $c_{ir}>0$ exactly when the arc curves to the right of the oriented connecting segment; and the number of sides n depends only on the cell.

The first theoretical assumption that we impose on our system of cells (cell aggregate) is:

Assumption 1: Our cell aggregate itself may be described as a "cell", i.e. a piecewise circular closed curve.

Physically, this means that the cell aggregate we are studying (1) cannot be broken up into two or more disconnected groups of cells, and (2) has no "holes". In mathematical terms, the cell aggregate (along with interiors) is simply connected. The usefulness of this assumption arises immediately in that we may associate the entire outside world with the exterior of a "cell" (piecewise circular closed curve) defined by the boundary of all the real cells in the system. We are led naturally to the following definition of the cell aggregate as a whole:

Definition: The mathematical system which we will associate with a group of m-1 natural cells is a collection of m cells $C_1, \ldots, C_m$ as defined above, where we arbitrarily associate the last cell with the outside world. We also adopt the convention that each curve in the system has a clockwise orientation, except for the outside world "cell", whose orientation is counterclockwise (see Fig. 2).

Our next assumption arises from the fact that interfaces are shared between two cells:

Assumption 2: The r^{th} side of the i^{th} cell C_i is the point set of the arc determined by v_{ir}, v_{ir+1} and the curvature c_{ir}. This side is equal as a point set to exactly one other side in the system (say the s^{th} side of cell C_j). With the conventions adopted above, we have

$$v_{ir} = v_{js+1}$$

$$v_{ir+1} = v_{js}$$

$$c_{ir} = -c_{js}$$

if both cells represent actual cells in the system, or

$$v_{ir} = v_{js}$$

$$v_{ir+1} = v_{js+1}$$

$$c_{ir} = c_{js}$$

if one is the outside world cell.

PHYSICAL RESTRICTION EQUATIONS

Having established the parameters and conventions we use to describe this system of cells, we now set out restrictions on the system represented by a set of equations which are based on explicit physical assumptions. Our goal here is to incorporate justifiable physical insight into the nature of a group of cells; specifically, conditions for equilibrium in the system for a given set of adhesive properties of the cells involved.

The plateau assumption

The first assumption about our system is the analogy of Plateau's theorem for soap bubbles. Plateau found that in stable systems of bubbles, junctions of more than three bubbles at a point were never observed. The physical justification for this phenomenon is a simple argument based on minimizing tensile surface energy for given volumes of bubbles. A full justification for the use of this assumption to model a given group of cells would require either an energy-minimizing argument that took into account the varying properties of membranes in the cell ensemble, or alternatively a simple empirical verification that the only junctions seen to occur in the system are three-way junctions. The importance of this point cannot be overemphasized: the Plateau assumption has far-reaching consequences in terms of the restriction equations of the model, and is central to the structure of the equations that follow.

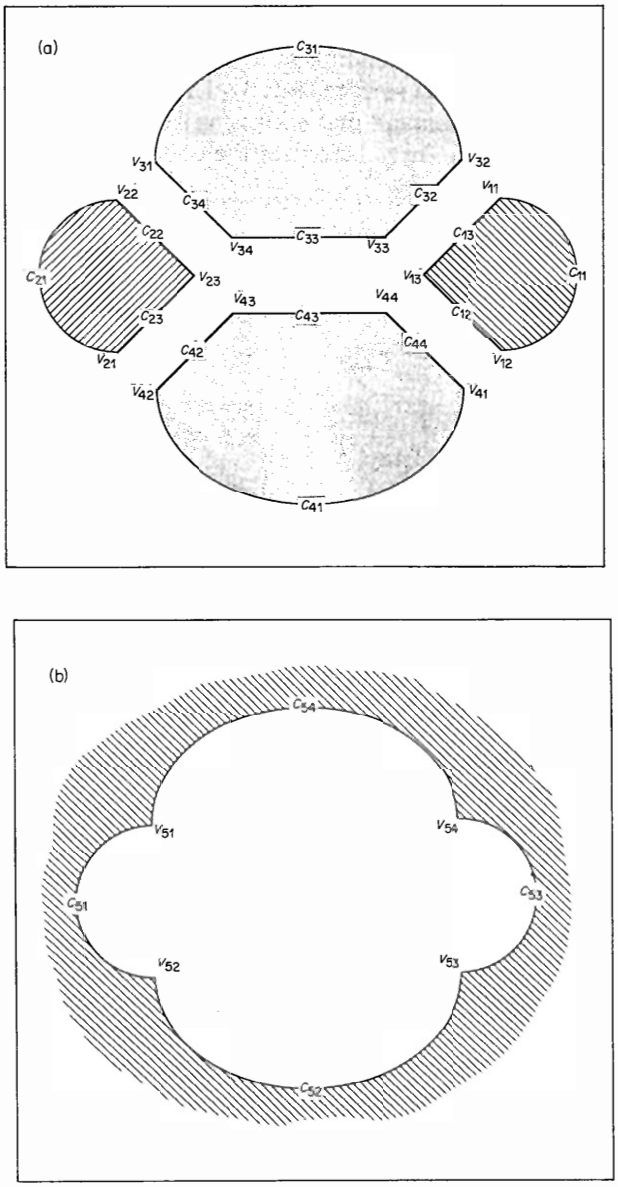

FIG. 2. Sample system of four cells with labeled vertices and side curvatures, plus the associated "outside world" cell.

To make use of the Plateau assumption, our model assumes that the curvature of a given contact between cells depends only on the cells, i.e. it is constant over the contact. As such it would be either redundant or physically unjustifiable to have a vertex v_{ir} of the system corresponding to a junction of only two cells, that is, falling in the middle of a contact surface (Fig. 3). Thus, in order to describe a given system of cells uniquely we demand that each vertex be the meeting point of three cells of the system, giving the formulation for the complete Plateau assumption:

Assumption 3: Each vertex v_{ir} in the system is a vertex of *exactly* three cells in the system, including the outside world.

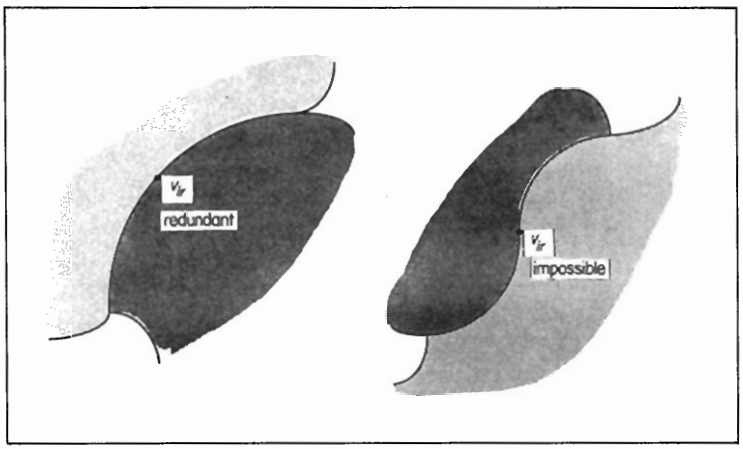

FIG. 3. Two unwanted vertex position possibilities that are eliminated with the plateau assumption.

The constant volume assumption

The next assumption we impose on the model is the analog of the fact that soap bubbles enclose a constant volume of air. While fluids inside cells are essentially incompressible, membranes are certainly permeable to many substances, and cells grow. However, our aim is to establish a set of restriction equations describing the equilibrium configuration of a conglomerate of cells *at a given point in time.* We thus assume that a cell retains a constant volume over the time it takes the system to reach a local energy minimum configuration. (Note that the appropriateness of this assumption must be determined for any particular implementation of the model by empirical testing.) With this in mind we state:

Assumption 4: The plane area of each cell in our system is exogenously determined.†

Stated in a general form, the expression for the area of a cell in our system is complex. However, in simple cases with a small number of cells, the form of the

† In our system this is equivalent to the constant volume assumption because the model treats an epithelium as two-dimensional, essentially assuming a constant depth.

restriction equations on the basic parameters of the model can be simplified considerably. We present here the general form of the restriction equations (Chichilnisky, 1985); section 5 of this paper presents a sample of simplified restriction equations in an explicit example of a cell configuration. In general, let us assume that:

(1) The sides of the polygon determined by the vertices of a cell do not cross over each other, and

(2) The circular arcs of each side of the cell do not intersect other arcs of the same cell.

Then if we write the horizontal and vertical coordinates of points as

$$v_{ir} = (v_{irx}, v_{iry})$$

$$v_{ir+1} = (v_{ir+1x}, v_{ir+1y}),$$

denoting the absolute value of a vector v by $\|v\|$, and setting $v_{in+1} = v_{i1}$ as a convention, then the area of the polygon determined by the vertices of the cell C_i is

$$PA_i = \sum_{j=1}^{n} x_r \|v_{ij}\| \|v_{ij+1}\| \sin [\arctan (v_{ir+1y}/v_{ir+1x}) - \arctan (v_{iry}/v_{irx})] \qquad (1)$$

where $x_r = -1$ if $v_{irx} \neq 0$ and $v_{iry}v_{ir+1x}/|v_{irx}| > v_{ir+1y}$ or $v_{irx} = 0$ and $v_{iry}v_{ir+1x} > 0$ and $x_r = 1$ otherwise.

To obtain the area of a given cell, we add or subtract the area of the circular segments to PA_i, depending on the sign of the curvature (see cell definition above). The expression for the area of a segment corresponding to a side is calculated as follows. Denoting the central angle associated with each circular arc by Ω_r, we have

$$\Omega_r = 2 \arcsin (c_{ir}\sqrt{[(v_{irx+1} - v_{irx})^2 + (v_{iry+1} - v_{iry})^2]}/2)$$

so that the area contribution SA_i of the circular segments is

$$SA_i = \sum x_r \operatorname{sgn} (c_{ir})(\Omega_r - \sin(\Omega_r))/2 \qquad (2)$$

and finally the total area A_i of the ith cell is simply

$$A_i = PA_i + SA_i. \qquad (3)$$

Thus our last model assumption about plane areas reduces to simply stating that the area A_i is determined exogenously for i between 1 and m.

Having formalized the Plateau assumption and the fixed volume assumption, we now present the tension equilibrium conditions for an energetically stable system.

Tension equilibrium assumption

As stated above, each vertex v_{ir} of our system corresponds to exactly two other vertices, that is, represents the meeting point of three cells. Consider each of the three-membrane contact surfaces meeting at the point $v_{ir} = v_{js} = v_{kt}$. The surface tension in each will cause it to exert a force in a direction tangential to the membrane surface at the junction point (see Fig. 4). Since this system is in dynamic equilibrium, the force vectors must sum to zero. In the case of soap bubbles, the homogeneity of the soap film forces the tensions in each surface to be roughly equal, meaning that each vertex has angles between tangent vectors of approximately 120°. In the

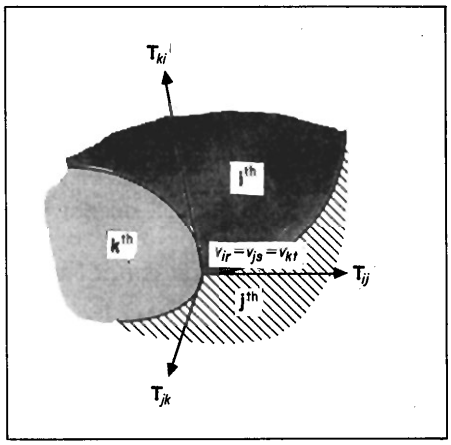

FIG. 4. Tangential pull of three membranes in dynamic equilibrium (forces cancel).

more complex case of cells, differing properties of distinct surfaces of contact allow tensions of unequal value to meet at a point, so that the equilibrium condition is more complex. Before formalizing these notions, we present

Assumption 5: The tensions of membranes at each three-way contact are in equilibrium, i.e. their vector sum is zero.

In the general case, consider three forces vectors $\mathbf{F}_1, \mathbf{F}_2$, and $\mathbf{F}_3$ meeting with opposite angles ϕ_1, ϕ_2, and ϕ_3 with vector sum zero (Fig. 5). For the vectors to cancel, the components of $\mathbf{F}_2$ and $\mathbf{F}_3$ in the direction perpendicular to $\mathbf{F}_1$ must cancel each other. Denoting the magnitudes of these vectors respectively by F_1, F_2, and F_3, we have

$$F_3 \sin(\phi_2) = F_2 \sin(\phi_3)$$

and similarly

$$F_3 \sin(\phi_1) = F_1 \sin(\phi_3)$$

so

$$F_1/\sin(\phi_1) = F_2/\sin(\phi_2) = F_3/\sin(\phi_3). \tag{4}$$

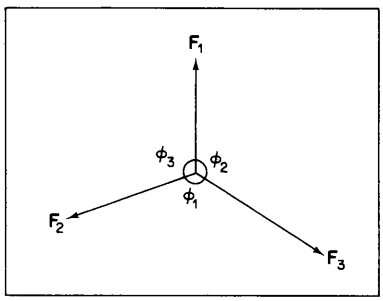

FIG. 5. Diagram for vector equilibrium equation derivation.

To adapt this equilibrium formula to the parameters of the model, consider three tensions T_{ij}, T_{jk}, and T_{ki} in equilibrium at the meeting point $v_{ir} = v_{js} = v_{kt}$. Let

$$d_{ir} = \sqrt{(c_{ir}^{-2} + [(v_{ir+1x} - v_{irx})^2 + (v_{ir+1y} - v_{iry})^2]/4)}$$

be the center-to-midpoint distance, and let

$$S_{ir} = (v_{iry} - v_{ir+1y},\ v_{ir+1x} - v_{irx})$$

be the perpendicular vector to the left of the oriented segment (Fig. 6). Then the center of curvature of the rth arc of the ith cell is given by

$$P_{ir} = (v_{ir} + v_{ir+1})/2 + d_{ir}(S_{ir}/\|S_{ir}\|)\ \mathrm{sgn}\ (c_{ir}). \tag{5}$$

and a vector R_{ir} tangent to the membrane surface at v_{ir} by

$$R_{ir} = (v_{iry} - P_{iry},\ P_{irx} - v_{irx}). \tag{6}$$

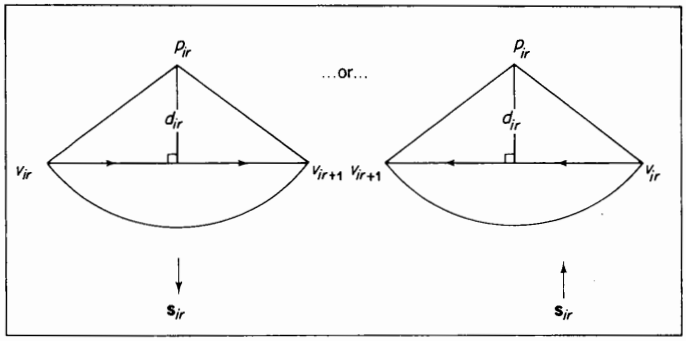

FIG. 6. Calculating the center of curvature of an arc.

Calculating R_{js} and R_{kt} analogously gives the tension vectors that must sum to zero

$$F_{ki} = T_{ki}R_{ir}/\|R_{ir}\| \tag{7}$$

$$F_{jk} = T_{jk}R_{kt}/\|R_{kt}\| \tag{8}$$

$$F_{ij} = T_{ij}R_{js}/\|R_{js}\| \tag{9}$$

for the associated tension equilibrium equation

$$F_{ki} + F_{jk} + F_{ij} = 0. \tag{10}$$

We have now established the formal restriction equations that represent the Plateau (three-way) assumption, the fixed volume assumption, and the tension equilibrium (stability) condition. We now turn to the pressure-tension assumption, the final basic physical restriction on our system that links the notions of membrane surface tension and interfacial curvature. This will allow us to use the adhesion input parameters of the model to solve for the curvature variables.

Pressure-tension equation

A membrane separating two chambers of a fluid has a curvature which is proportional to the difference in pressure between the two chambers, and inversely proportional to the tension in the surface of contact (Childress & Percus, 1978). That is, a high pressure differential between the chambers will cause the separating membrane to curve more, and a high tension in the membrane will counteract this tendency by flattening the membrane (Fig. 7).

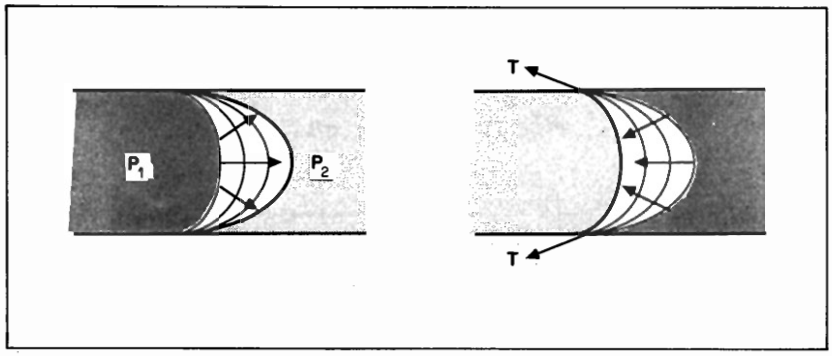

FIG. 7. The pressure-tension equation. If $\mathbf{P}_1 \gg \mathbf{P}_2$ then the curvature of the separating membrane will be larger. Also, a higher tension **T** will tend to decrease the curvature of the separating membrane.

By considering the pressures of the fluids inside each cell in our system to also be parameters of the model, we can then link the membrane surface tension and the membrane curvature:

Assumption 6: Let us associate with each cell C_i in our system a real number P_i that represents the pressure of the fluid inside the cell. If C_i shares its rth side with a cell C_j on its sth side, then we have

$$P_i - P_j = T_{ij}c_{ir} \tag{11}$$

where T_{ij} represents the surface tension in the i-j contact. Noting our sign conventions, this is equivalent to saying

$$P_j - P_i = T_{ij}c_{js} \tag{12}$$

(unless $j = m$, in which case $P_i - P_j = T_{ij}c_{js}$). Also, P_m has a physical interpretation as the pressure of the surrounding world.

This formalizes the link between tensions and curvatures in our system. The equation above with the form $\Delta P = TC$ links a curvature parameter to an internal pressure, via the exogenous parameter T. However, for any given cell the pressure term in the equation that corresponds to each of the n sides of the cell remains the same, so in fact these equations for any one cell relate all the curvatures to each other, and thus aid in solving for them.

Having explicitly written out all the physical restrictions on our system of cells, we are now in a position to incorporate Steinberg's differential adhesion hypothesis and examine how to make use of all the machinery that has been established.

THE DIFFERENTIAL ADHESION HYPOTHESIS

Until now, the physical assumptions in this model have dealt mostly with the soap-bubble analogy, except for a more general treatment of tension equilibrium. We now wish to show why this more general treatment of surface tension in fact allows us to bring into play the question of adhesivity. The important insight here is:

Assumption 7: The surface tension in a cell-cell contact is a function of the strength of adhesion of the contact.

The relationship between the adhesion and the tension in a contact arises from a need to balance forces at the junction points. If w_{ii}, w_{jj}, and w_{ij} are the works of cohesion per unit of surface area respectively in contacts between cell types i and i, j and, j, and i and j, the surface tension in a contact between cells of types i and j is given by

$$T_{ij} = (w_{ii} + w_{jj})/2 - w_{ij}.$$

A derivation of this equality relating the tension of a contact to the adhesive properties of the cells involved is presented in Childress & Percus (1978).

If we consider the differing adhesion values between cells (works of cohesion per unit surface area) to be the principal modeling inputs, then we can use a formulation to calculate directly from these values the membrane tension in each contact. The usefulness of this relationship now becomes apparent. With it, we will henceforth treat adhesion and tension as the same exogenous parameter T_{ij} in our model for any given surface of contact. To incorporate Steinberg's differential adhesion hypothesis, we simply state that

Assumption 8: The tension (adhesion) T_{ij} in the surface of contact of cells C_i and C_j is an exogenous parameter that depends only on the two cells involved.

So far the only exogenous parameters in the model have been (1) the fixed areas of the cells involved, and now (2) the tension (adhesion) of each contact. With this in mind, we now set out to establish the existence of an equilibrium configuration of the system, i.e., equilibrium values of all the parameters simultaneously, with areas and adhesive strengths as the only inputs. If cell areas and adhesive strengths of contact between cells are known, a solution of the model will predict exactly the configuration of the system of cells being studied.

3. Solving the Model: Equilibrium solutions

In order to determine the existence of an equilibrium and implement the model, we begin by summarizing the parameters and restriction equations.

The endogenous parameters of the model are the variables which describe the m "cells" in a given system. Each cell C_i is said to have $n(i)$ vertices (points) and

curvature variables as well as one pressure value associated with it. Let $N = \sum n(i)$, the total number of vertices (or sides) described in the system. The *endogenous parameter* list consists of:

(1) $2N$ real numbers of the form v_{irx} and v_{iry} describing the vertices.

(2) N real numbers of the form c_{ir} describing curvatures.

(3) m real numbers written P_i corresponding to internal cell pressures.

The *exogenous parameters* (or "input values") of the model are:

(1) m real numbers written A_i corresponding to cell volumes.

(2) real numbers T_{ij} corresponding to the tension in each i–j contact.

The first step in solving the model involves the question of cell contacts. In the discussion of the Plateau assumption above, we noted that each vertex of each cell in the system corresponded to exactly two other vertices in the system, generating equations of the form $v_{ir} = v_{js} = v_{kt}$, which we will call "contact equations". The assumption that the cells be oriented clockwise except for the "outside world" cell further shows that these vertex equalities would generate curvature equalities, for example $c_{ir} = c_{kt-1}$, $c_{js} = c_{ir-1}$, and $c_{kt} = c_{js-1}$ in Fig. 4. In fact, it is clear that a complete set of such vertex equalities establishes a cell-contact pattern for the entire system.

The assumption of three-way intersections throughout the system has far-reaching consequences. For example, it is easy to show that for a system of three cells or four cells there is only one such possible configuration (Chichilnisky, 1985). In the general case, the Plateau assumption places severe constraints on the cell contact pattern, to the point that for small numbers of cells we can expect to find all configurations of the system quite easily by testing out different contact equations. It is also worth noting that not all sets of cell-contact equations can exist in the plane; in the general case we will be able to generate topologically nontrivial surfaces that have no meaning in this model by simply specifying a set of equations of the form $v_{ir} = v_{js} = v_{kt}$.

Let us suppose a full set of contact equations to exist for a given system of cells. We now set out to show that an equilibrium configuration for the system exists, i.e. that from the contact equations and the tension and area inputs, we may explicitly solve for all the endogenous variables in the system, and thereby obtain a *complete predicted picture* in two dimensions of the system we are studying, based on the theoretical assumptions above.

For each vertex variable v_{ir} there is one contact equation of the form $v_{ir} = v_{js} = v_{kt}$. These equations together describe the entire set of cell contacts of the system. Similarly, each curvature c_{ir} has a corresponding equation $c_{lu} = c_{mv}$, which can be derived from the vertex equalities. These equalities reduce the number of free vertex variables by two-thirds, and the number of free curvature variables by one-half, leaving the following *free endogenous variables*:

(1) $2N/3$ real numbers of the form v_{irx} and v_{iry} describing the vertices.

(2) $N/2$ real numbers of the form c_{ir} describing curvatures.

(3) m real numbers written P_i corresponding to internal cell pressures.

Now let us examine more carefully our restriction equations. The tension-equilibrium assumption provides a vector equality of the form $\mathbf{F}_{ki} + \mathbf{F}_{jk} + \mathbf{F}_{ij} = 0$ from equations (4)-(10) for each *distinct* vertex of the system, i.e. for each actual meeting

point of three contact surfaces, which number $N/3$. Note that each vector equality in two dimensions actually represents two independent equations. Exactly one of these vector equations is dependent on the others, for when the angles of contact of the system have been found explicitly except for those at one last vertex, the angles at this last vertex will clearly be determined by the incoming membranes from other points. This leaves $2N/3$-2 equations.

The pressure-tension assumption generates an independent constraint equation of the form $\Delta P = TC$ from equations (11) and (12) for each distinct surface of contact (wall) in the system, which number $N/2$ since each side of a cell corresponds exactly to one side of one other cell.

Finally, the constant area assumption generates an independent equation of the form $A_i = \text{const.}$ from equations (1)-(3) for each of the m cells in the system, except for the "outside world cell", whose interior volume is just the sum of all the others. Summarizing the restriction equations on our system:

(1) Tension Equilibrium:	$2N/3-2$	equations [from (4)-(10)].
(2) Pressure-Tension:	$N/2$	equations [from (11-(12)].
(3) Constant Area:	$m-1$	equations [from (1)-(3)].

By comparing this to the list of free endogenous variables, we obtain the correspondence:

(1) Tension Equilibrium:	$2N/3-2$	vs	$2N/3$	Vertex Variables.
(2) Pressure-Tension:	$N/2$	vs	$N/2$	Curvature Variables.
(3) Constant Area:	$m-1$	vs	m	Pressure Variables.

This result has several important implications.

In (1), the implication seems to be that the vertices (triple contacts) of a system of cells depend upon the tensions in the joining membrane. This is appealing, we can imagine an array of points joined by elastic bands of varying strength with an exterior force pulling out in all directions, the positions of the points being determined by relative strengths of the elastic bands pulling on them.† From (2) we see that indeed the curvatures are determined by exactly what we thought they should be: the pressure differential across and the tension in each contact surface. And finally, we have a very plausible relationship between the volume of each cell and the pressure of the interior fluids.

However, three equations seem to be missing: there are three more free variables in the system than restriction equations. The physical interpretation of this is simple: the way our system has been developed, our variables should be determined only up to translation and rotation in the plane. This is because in the physical analysis, only relative positions of points were used. More obviously, a cell conglomerate should adopt a given configuration irrespective of where it is in the world. Since translation involves two degrees of freedom (horizontal and vertical) and rotation

† Note: this interpretation is not precise and is only intended to give an intuitive picture of the forces at work. A soap film can behave transiently as an elastico-viscous liquid (Almgren & Taylor, 1976).

one (angle), we see that in fact the three additional degrees of freedom are completely justified and, in fact, expected.

4. Practical Examples: Systems of Three and Four Cells

To make explicit the implementation of this model in a concrete case, we carry out the steps for applying the equations to the cases of three and four cells.

First consider a group of three cells. By the Plateau assumption, we see immediately that each cell must share at least contact with each of the other two cells, and one with the environment. Leaving aside any highly irregular configurations, we conclude that the obvious contact configuration to study in the three-cell case is the one depicted in Fig. 8. For the four-cell case, it is easily shown (Chichilnisky, 1985) that all possible configurations which satisfy the Plateau assumption are of the form that shown in Fig. 9, where only the identities of the cells in the picture may vary. This allows for exactly 6 configurations in the four cell case.

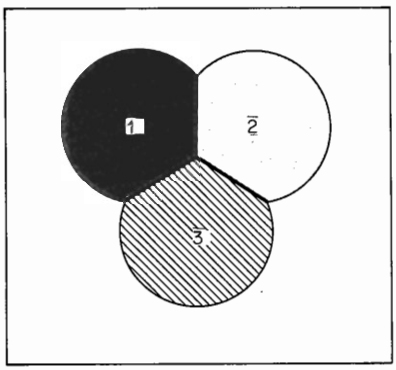

FIG. 8. The general contact configuration possibility in the three-cell case

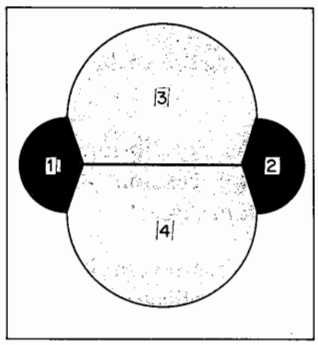

FIG. 9. The general contact configuration possibility in the four-cell case.

As we have just seen, at least in small numbers of cells, the Plateau assumption of three-way contacts places severe limitations on the possible configurations of a system of cells, and thus simplifies considerably the task of checking the space of all such configurations. In the three- and four-cell cases, there is only one (reasonable) form of contact configuration. We now show how, having established the contact configuration, we may move directly to calculating an explicit numerical solution of the positions, sizes, and shapes of the cells in two dimensions.

First, we apply the notation introduced above. We describe each vertex of the system by a point variable v_i, and the curvature of each side by a real variable c_i, as in Fig. 10. We have 12 vertices, for a total of 24 real variables, 12 real curvature variables, and 4 real presure variables, giving 40 endogenous parameters. We also assign the tension (adhesion) exogenous parameter T_{ij} to the contact between the ith and jth cells, $i<j$.

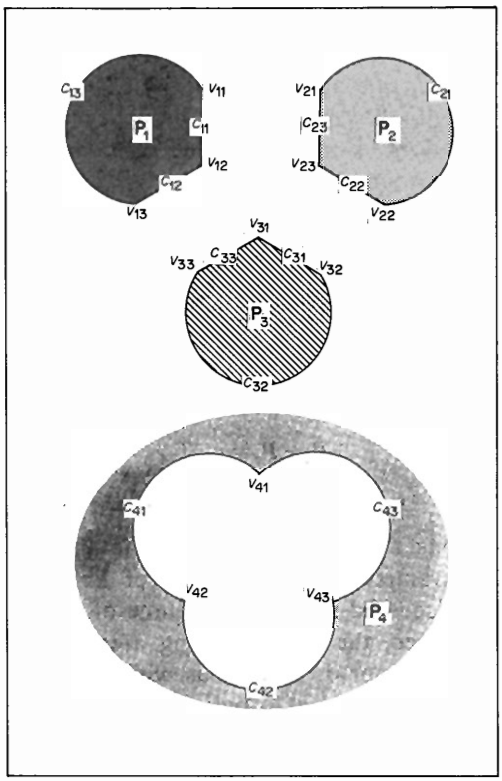

FIG. 10. Defining explicitly the vertices and curvatures of our three-cell system.

Denoting by v_{irx} and v_{iry} respectively the horizontal and vertical elements of the point v_{ir}, we write out the contact equations described by the figure, which equate corresponding vertex and curvature variables.

Contact Equations:

$$v_{11x} = v_{21x} = v_{41x} \quad \text{and} \quad v_{11y} = v_{21y} = v_{41y}$$

$$v_{22x} = v_{32x} = v_{43x} \quad \text{and} \quad v_{22y} = v_{32y} = v_{43y}$$

$$v_{13x} = v_{33x} = v_{42x} \quad \text{and} \quad v_{13y} = v_{33y} = v_{42y}$$

$$v_{12x} = v_{23x} = v_{31x} \quad \text{and} \quad v_{12y} = v_{23y} = v_{31y}$$

$$c_{11} = -c_{23}$$

$$c_{22} = -c_{31}$$

$$c_{33} = -c_{12}$$

$$c_{13} = c_{41}$$

$$c_{21} = c_{42}$$

$$c_{32} = c_{43}$$

Noting that each triple equality yields two distinct equations, we obtain 18 initial restriction equations.

Next we obtain one pressure-tension equation as shown above and in (11) and (12) for each distinct cell-cell contact. This yields 6 restriction equations on the system in terms of exogenous tension (adhesion) parameters and endogenous pressure and curvature parameters.

Pressure-Tension Equations:

$$P_1 - P_2 = c_{11} T_{12}$$
$$P_2 - P_3 = c_{22} T_{23}$$
$$P_3 - P_1 = c_{33} T_{13}$$
$$P_1 - P_4 = c_{13} T_{14}$$
$$P_2 - P_4 = c_{21} T_{24}$$
$$P_3 - P_4 = c_{32} T_{34}$$

Next we apply the Constant Volume assumption to obtain corresponding restriction equations on the parameters. We set the area of the three "real" cells to be A_1, A_2, and A_3. Since, as discussed above, the volume of the "outside world" cell is the sum of the other three, the corresponding area restriction equation is not independent, and is thus ignored, leaving us with three independent restriction equations. We do not use the general polygon area formula described in equation (1) for the triangles, rather, we take advantage of the simplicity of triangles to clean up the equations.

Area Equations:

Cell 1.

$$\text{Let} \quad a_1 = \sqrt{(v_{11x} - v_{12x})^2 + (v_{11y} - v_{12y})^2}$$
$$b_1 = \sqrt{(v_{12x} - v_{13x})^2 + (v_{12y} - v_{13y})^2}$$
$$c_1 = \sqrt{(v_{13x} - v_{11x})^2 + (v_{13y} - v_{11y})^2}$$

$$\begin{aligned}\text{AREA}_1 = {} & (a_1/2)\sqrt{[b_1^2 - (a_1^2 + b_1^2 - c_1^2)^2/4a_1^2]} \\ & + \text{sgn}\,(c_{11})[\arcsin\,(c_{11}a_1/2)/c_{11}^2 - (a_1/2)\sqrt{(c_{11}^2 - a_1^2/4)}] \\ & + \text{sgn}\,(c_{12})[\arcsin\,(c_{12}b_1/2)/c_{12}^2 - (b_1/2)\sqrt{(c_{12}^2 - b_1^2/4)}] \\ & + \text{sgn}\,(c_{13})[\arcsin\,(c_{13}c_1/2)c_{13}^2 - (c_1/2)\sqrt{(c_{13}^2 - c_1^2/4)}] \\ = {} & A_1\end{aligned}$$

Similarly, for the other two cells we have:

Cell 2.

$$\text{Let} \quad a_2 = \sqrt{(v_{21x} - v_{22x})^2 + (v_{21y} - v_{22y})^2}$$
$$b_2 = \sqrt{(v_{22x} - v_{23x})^2 + (v_{22y} - v_{23y})^2}$$
$$c_2 = \sqrt{(v_{23x} - v_{21x})^2 + (v_{23y} - v_{21y})^2}$$

$$\begin{aligned}\text{AREA}_2 &= (a_2/2)\sqrt{[b_2^2-(a_2^2+b_2^2-c_2^2)^2/4a_2^2]}\\ &\quad+\operatorname{sgn}(c_{21})[\arcsin(c_{21}a_2/2)/c_{21}^2-(a_2/2)\sqrt{(c_{21}^2-a_2^2/4)}]\\ &\quad+\operatorname{sgn}(c_{22})[\arcsin(c_{22}b_2/2)c_{22}^2-(b_2/2)\sqrt{(c_{22}^2-b_2^2/4)}]\\ &\quad+\operatorname{sgn}(c_{23})[\arcsin(c_{23}c_2/2)/c_{23}^2-(c_2/2)\sqrt{(c_{23}^2-c_2^2/4)}]\\ &= A_2\end{aligned}$$

Cell 3.

$$\begin{aligned}\text{Let}\quad a_3 &= \sqrt{(v_{31x}-v_{32x})^2+(v_{31y}-v_{32y})^2}\\ b_3 &= \sqrt{(v_{32x}-v_{33x})^2+(v_{32y}-v_{33y})^2}\\ c_3 &= \sqrt{(v_{33x}-v_{31x})^2+(v_{33y}-v_{31y})^2}\end{aligned}$$

$$\begin{aligned}\text{AREA}_3 &= (a_3/2)\sqrt{[b_3^2-(a_3^2+b_3^2-c_3^2)^2/4a_3^2]}\\ &\quad+\operatorname{sgn}(c_{31})[\arcsin(c_{31}a_3/2)/c_{31}^2-(a_3/2)\sqrt{(c_{31}^2-a_3^2/4)}]\\ &\quad+\operatorname{sgn}(c_{32})[\arcsin(c_{32}b_3/2)/c_{32}^2-(b_3/2)\sqrt{(c_{32}^2-b_3^2/4)}]\\ &\quad+\operatorname{sgn}(c_{33})[\arcsin(c_{33}c_3/2)/c_{33}^2-(c_3/2)\sqrt{(c_{33}^2-c_3^2/4)}]\\ &= A_3.\end{aligned}$$

With the volume constraint in place, we now formalize the tension equilibrium equations for our three-cell system. Since one vector equality holds at each of the four distinct vertices in the picture, and since one of these vector equalities is dependent, we are left with a total of 6 distinct restriction equations.

Tension Equilibrium Equations:

Top Vertex (Fig. 10).

$$\begin{aligned}\text{Let}\quad d_{11} &= \sqrt{(c_{11}^{-2}+[(v_{12x}-v_{11x})^2+(v_{12y}-v_{11y})^2]/4)}\\ S_{11} &= (v_{11y}-v_{12y},\, v_{12x}-v_{11x})\\ d_{21} &= \sqrt{(c_{21}^{-2}+[(v_{22x}-v_{21x})^2+(v_{22y}-v_{21y})^2]/4)}\\ S_{21} &= (v_{21y}-v_{22y},\, v_{22x}-v_{21x})\\ d_{41} &= \sqrt{(c_{41}^{-2}+[(v_{42x}-v_{41x})^2+(v_{42y}-v_{41y})^2]/4)}\\ S_{41} &= (v_{41y}-v_{42y},\, v_{42x}-v_{41x})\\ P_{11} &= (v_{11}+v_{12})/2+d_{11}(S_{11}/\|S_{11}\|)\operatorname{sgn}(c_{11})\\ P_{21} &= (v_{21}+v_{22})/2+d_{22}(S_{21}/\|S_{21}\|)\operatorname{sgn}(c_{21})\\ P_{41} &= (v_{41}+v_{42})/2+d_{41}(S_{41}/\|S_{41}\|)\operatorname{sgn}(c_{41})\\ R_{11} &= (v_{11y}-P_{11y},\, P_{11x}-v_{11x})\\ R_{21} &= (v_{21y}-P_{21y},\, P_{21x}-v_{21x})\\ R_{41} &= (v_{41y}-P_{41y},\, P_{41x}-v_{41x})\end{aligned}$$

$$T_{14}R_{11}/\|R_{11}\|+T_{12}R_{21}/\|R_{21}\|+T_{24}R_{41}/\|R_{41}\|=0$$

Leftmost Vertex (Fig. 10).

$$
\begin{aligned}
\text{Let}\quad & d_{13} = \sqrt{(c_{13}^{-2} + [(v_{11x} - v_{13x})^2 + (v_{11y} - v_{13y})^2]/4)} \\
& S_{13} = (v_{13y} - v_{11y},\ v_{11x} - v_{13x}) \\
& d_{33} = \sqrt{(c_{33}^{-2} + [(v_{31x} - v_{33x})^2 + (v_{31y} - v_{33y})^2]/4)} \\
& S_{33} = (v_{33y} - v_{31y},\ v_{31x} - v_{33x}) \\
& d_{42} = \sqrt{(c_{42}^{-2} + [(v_{43x} - v_{42x})^2 + (v_{43y} - v_{42y})^2]/4)} \\
& S_{42} = (v_{42y} - v_{43y},\ v_{43x} - v_{42x}) \\
& P_{13} = (v_{13} + v_{11})/2 + d_{13}(S_{13}/\|S_{13}\|)\ \operatorname{sgn}(c_{13}) \\
& P_{33} = (v_{33} + v_{31})/2 + d_{33}(S_{33}/\|S_{33}\|)\ \operatorname{sgn}(c_{33}) \\
& P_{42} = (v_{42} + v_{43})/2 + d_{42}(S_{42}/\|S_{42}\|)\ \operatorname{sgn}(c_{42}) \\
& R_{13} = (v_{13y} - P_{13y},\ P_{13x} - v_{13x}) \\
& R_{33} = (v_{33y} - P_{33y},\ P_{33x} - v_{33x}) \\
& R_{42} = (v_{42y} - P_{42y},\ P_{42x} - v_{42x}) \\
& T_{11}R_{13}/\|R_{13}\| + T_{43}R_{33}/\|R_{33}\| + T_{14}R_{42}/\|R_{42}\| = 0
\end{aligned}
$$

Rightmost Vertex (fig. 10).

$$
\begin{aligned}
\text{Let}\quad & d_{32} = \sqrt{(c_{32}^{-2} + [(v_{33x} - v_{32x})^2 + (v_{33y} - v_{32y})^2]/4)} \\
& S_{32} = (v_{32y} - v_{33y},\ v_{33x} - v_{32x}) \\
& d_{22} = \sqrt{(c_{22}^{-2} + [(v_{23x} - v_{22x})^2 + (v_{23y} - v_{22y})^2]/4)} \\
& S_{22} = (v_{22y} - v_{23y},\ v_{23x} - v_{22x}) \\
& d_{43} = \sqrt{(c_{43}^{-2} + [(v_{41x} - v_{43x})^2 + (v_{41y} - v_{43y})^2]/4)} \\
& S_{43} = (v_{43y} - v_{41y},\ v_{41x} - v_{43x}) \\
& P_{32} = (v_{32} + v_{33})/2 + d_{32}(S_{32}/\|S_{32}\|)\ \operatorname{sgn}(c_{32}) \\
& P_{22} = (v_{22} + v_{23})/2 + d_{22}(S_{22}/\|S_{22}\|)\ \operatorname{sgn}(c_{22}) \\
& P_{43} = (v_{43} + v_{41})/2 + d_{43}(S_{43}/\|S_{43}\|)\ \operatorname{sgn}(c_{43}) \\
& R_{32} = (v_{32y} - P_{32y},\ P_{32x} - v_{32x}) \\
& R_{22} = (v_{22y} - P_{22y},\ P_{22x} - v_{22x}) \\
& R_{43} = (v_{43y} - P_{43y},\ P_{43x} - v_{43x}) \\
& T_{23}R_{32}/\|R_{32}\| + T_{24}R_{22}/\|R_{22}\| + T_{34}R_{43}/\|R_{43}\| = 0.
\end{aligned}
$$

5. Implementing the Model: the Effect of Varying Adhesions

Having carried out an explicit equilibrium solution of the model for the case of three cells, we now describe how to implement the model in the general case. If applied in the way outlined below, the model may be used to apply energy-minimizing principles as a way of describing the dynamics of morphogenesis.

First let us consider the question of minimizing energy. It is a well-studied phenonenon (Plateau, 1873; Thompson, 1917; Almgren & Taylor, 1976) that soap-bubble conglomerates assume certain configurations in the interest of minimizing surface free energy. In soap bubbles, this free energy is the manifestation of the surface tension the soap film. Since the tension is essentially constant over the entire soapy film, the energy may be computed as simply the total area of the soap film in the bubble mass multiplied by a constant.

Similarly, we may compute a measure of the free energy of a system of cells by summing the energy of tension (adhesion) in the membranes. Since the adhesion is assumed to remain constant over a contact between any two given cells, this generalization of the soap bubble energy calculation remains simple, involving a discrete sum over the distinct surfaces of contact in the system. More precisely, let L_{ir} denote the length of the rth side of the ith cell, and let us say that at this side cell C_i contacts cell C_j. Then if we write the tension (adhesion) of the i–j contact as T_{ij}, the surface free energy of this membrane segment is given by $T_{ij}L_{ir}$. As we sum the free energy contributions over all sides in our cell aggregate, each side is duplicated once (see Assumption 2) so we obtain the following expression for the free energy of the system:

$$E = \sum T_{ij}L_{ir}. \tag{13}$$

We can now examine all possible configurations of the model, and find which of these has the lowest free-energy.

Take a small number of cells. We have already seen that the number of possible contact configurations (i.e. sets of equations such as $v_{ir} = v_{js} = v_{kt}$ listing the contacts of each cell) is reduced significantly by the Plateau assumption. For each such contact configuration, we have seen that it is possible to compute a precise predicted equilibrium "drawing" of the system, using as inputs only the intracellular tension (adhesion) values, and the cell volumes. Once such an equilibrium value is computed, we may apply equation (13) directly to the final picture and compute the energy associated with each contact configuration. One may then simply minimize over this discrete set of equilibrium energy values to find the most energetically favorable configuration of the system. The procedure is described diagramatically in Fig. 11.

In summary, the model allows us to predict fully and precisely the most likely configuration of a system of cells of given volume knowing only the intracellular adhesions.

Once such a static calculation of minimum energy has been carried out, it is a simple step to use the model to describe the dynamics of morphogenesis. If intracellular adhesion values are considered as real functions of time, then we can imagine calculating a series of "snapshots" of the system, where the ith snapshot is based

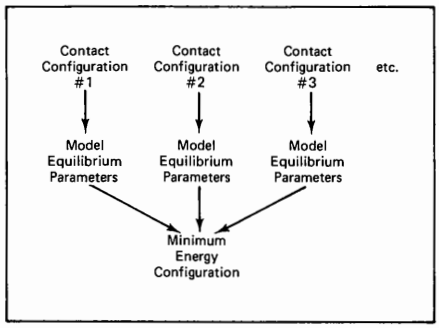

FIG. 11. Procedure for isolating most energetically favorable pattern of cells.

on the adhesion values at a time t_i. We are in effect assuming that morphology will track slowly varying adhesive parameters with a continuous series of equilibrium configurations. In this way, one could observe dynamically the effect of time dependent adhesion values (i.e. during development) on the movement and shaping of cells as a way of understanding morphogenesis and pattern formation.

6. Summary

In summary, the model is theoretically simple. We have presented the following assumptions about the physical nature of a system of cells:

Plateau Assumption (3-Way Junctions)
Fixed Volume Assumption
Pressure–Tension Assumption
Tension Equilibrium Assumption.

These simple and justifiable axioms allow us to compute a complete equilibrium picture associated with a given set of cell contacts, using as inputs the volumes of the cells and intracellular adhesion values. From this picture we move easily to an energy calculation associated with the given set of contacts. Repeating the same procedure over all reasonable contact possibilities yields a most energetically favorable configuration of the system, i.e. a predicted picture of the system, based only on volumes and adhesive strengths. If adhesions are understood to vary over time, we can observe the predicted effect of time dependent adhesion values as a mechanism for pattern formation.

The advantage of this approach is fourfold. First, it allows us to use the concept of differential adhesion to predict cell contacts and shapes, based on an energy-minimizing principle, in a way that respects the subtleties of cell deformation. Second, the explicitness of the output from the model allows for direct simulation and testing of its hypothesis. Third, the model can be applied in a natural way to study changing cell configurations over time. Finally, it provides a mechanism for understanding at a deep level the effects of differential membrane adhesivity on cell shapes and contacts, and on the dynamics of pattern formation.

REFERENCES

ALMGREN, F. J. & TAYLOR, J. E. (1976). *Sci. Am.* **235,** 82.
CHICHILNISKY, E. J. (1985). Senior Thesis, Department of Mathematics, Princeton University.
CHILDRESS, S. & PERCUS, J. K. (1978). *Mathematical Models in Development Biology.* New York: Courant Institute of Mathematical Sciences.
GOEL, R. G. NARENDRA, S., STEINBERG, M. S., & WEISMAN, L. (1972). *J. theor. Biol.* **37,** 43.
HONDA, H. (1983). *Int. Rev. Cytol.* **81,** 191.
MITTENTHAL, J. E. & MAZO, R. M. (1983). *J. theor. Biol.* **100,** 443.
NARDI, J. B. & KAFATOS, S. (1976). *J. Embryol. Exp. Morphol.* **36,** 489.
PLATEAU, J. A. F. (1873). *Statique Experimentale et Theorique des Liquides Soumis aux Seules Forces Moleculaires.* Paris: Gauthier.
STEINBERG, M. S. (1962). *Science* **137,** 762.
STEINBERG, M. S. (1978). *Cell-Cell Recognition in Multicellular Assembly: Levels of Specificity.* Cambridge University Press: Society for Experimental Biology Symposium.
SULSKY, D. (1984). *J. theor. Biol.* **106,** 275.
THOMPSON, D. (1917). *On Growth and Form.* Cambridge University Press.